Pacific Marine Mammal Center

Case Reports in Marine Mammal Pathology
Volume 1, Number 1, March 2014

Simultaneous Hypo- and Hyper-Metabolic Insults: Effects on Protein Loss and Survival in Advanced Malnutrition (Starvation)

Dennis F. Lawler DVM, FNAP; Basil P. Tangredi DVM; Richard H. Evans DVM, MS, FNAP

Abstract

A stranded juvenile Northern Elephant Seal was admitted to the Pacific Marine Mammal Center, Laguna Beach CA, with clinical and biochemical condition suggesting starvation. Rehydration and supportive nutritional therapy were initiated. A mass appeared on the mid-thoracic dorsum on day 9, and infrared photographic analysis suggested abscess, which was treated. On post-admission day 18, weakness, partial anorexia, and a dyspneic episode were observed. Laboratory evaluation indicated severe inflammation and tissue damage. Deterioration continued despite both specific and supportive treatment, and humane euthanasia was elected on day 23. Necropsy evaluation revealed cellulitis resulting from the earlier abscess, pneumonia, and signs consistent with acute congestive heart failure secondary to starvation-related cardiomyopathy. The effort to save this young elephant seal yielded a quantity of information that allowed thorough review of the course toward an inevitable mortality related to simultaneous occurrence of hypometabolic (starvation) and hypermetabolic (panniculitis and pneumonia) insults that negatively influenced a number of metabolic processes, especially protein balance. This case report demonstrates the need to consider all aspects of starvation, in order to more fully understand its pathobiology in marine mammals.

Introduction

Primary starvation is a common occurrence in young, stranded Northern Elephant seals (*Mirounga angustirostris*) and California sea lions (*Zalophus californianus*) admitted to Pacific Marine Mammal Center (PMMC) in Laguna Beach, California. Starving seals often present with concurrent, complicating disorders such as infections, excessive parasitism, and trauma. The process of differential diagnosis should include thorough postmortem evaluation of mortalities, and efforts to elucidate relationships among observed problems. Collations of these data can help segregate primary and secondary insults, and support identifying contributing environmental problems. The ultimate goals include providing optimal individual health care in rehabilitation, acting to prevent sometimes-inadvertent human-caused problems in aquatic ecologies, and recognizing effects of large-scope influences such as climate change. We present an example of complicated advanced starvation, demonstrating evaluations and differential pathological diagnosis of multiple effects in a young mammal.

History

On April 14th, 2012, a juvenile Northern Elephant Seal ("Dovahkin", M-12-04-14-034) was found stranded at Dana Point, California. The seal was impounded and transported to PMMC, where physical examination revealed it to be quiet, alert, reactive, and moderately underweight (49 kg), with dry and moderately crusted eyelids. Heart rate was 128 bpm, respiratory rate 12/min, body temperature was normal, mucous membranes were pink, capillary refill time (CRT) was 2.0-3.0 seconds. Serum glucose was low-normal (96 mg/dl). Resuscitative fluid (subcutaneous) and nutritional therapy (gastric lavage) were initiated.

The following day, blood was taken from the epidural sinus of the lumbar spine for complete blood count (CBC) and serum chemistry profile. CBC revealed absolute neutrophilia and marked lymphopenia, consistent with both malnutrition and

physiological stress response. Serum chemistry revealed markedly elevated creatine kinase (CK) and gamma-glutamyl transferase (GGT) and mildly depressed total protein, also consistent with advanced malnutrition (starvation) (Table 1).

Over the next 8 days, the seal was rehydrated and fed a moderately high-calorie diet by gastric intubation, along with daily subcutaneous fluid administration. On day 9, offered herring also was taken; by day 12, the seal was able to dive for food as well. However, the expected return of physical strength following rehydration and re-feeding was delayed.

On day 9, a 3 x 5cm ovoid cutaneous mass was noted on the mid-thoracic dorsum (Figure 1). Infrared photographic analysis (FLIR® camera) of the wound and surrounding skin (~10-15cm) registered temperature several degrees higher than normal, indicating inflammation (Figure 2). On day 12, enlarging of the mass precipitated aspiration, yielding minimal blood tinged fluid. On day 13, local anesthesia was administered, and the mass was opened to reveal a 1-2 cm subcutaneous pocket of red-tinted fluid, surrounded by moderate tissue necrosis and a small quantity of thick, grey exudate. A section of the lesion was taken for cytologic examination. The wound was suspected to be the result of subcutaneous contamination during fluid-therapy, and the area was debrided, cleansed and left open to drain. Amoxicillin-clavulanic acid was prescribed, and daily treatment was continued as the abscess healed, but appetite and activity nonetheless remained somewhat depressed.

On day 18, the seal experienced temporary dyspnea during a feeding attempt that was not pursued until later in the day. On day 19, he was partly anorectic and notably more weakened. Amikacin was added to the antibiotic regimen, and blood was taken for CBC and serum chemistry profile (Table 1). The day 19 CBC (Table 1) revealed mildly elevated red blood cells (RBC), hemoglobin (HGB), and mean cell hemoglobin concentration (MCHC), marked leukocytosis, moderate relative and absolute neutrophilia, marked relative and absolute band neutrophilia, moderate-to-marked relative and absolute lymphopenia, moderate-to-marked relative and absolute monocytosis, and marked thrombocytopenia. The CBC was consistent with severe inflammation. The serum chemistry profile revealed marked elevation of alanine transferase (ALT), aspartate transferase (AST), CK, and GGT, consistent with inflammation and tissue damage. Hyponatremia, hypoglycemia, hypocalcaemia, and hyperbilirubinemia also were observed.

Figure 1. Wound on central thoracic dorsum, following opening, debriding and cleaning

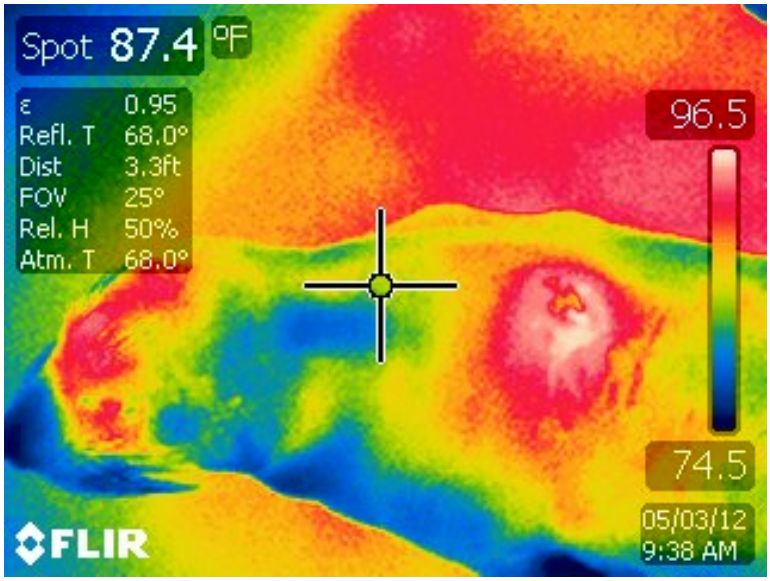

Figure 2. FLIR infra-red examination of thoracic dorsum wound. Note significant cutaneous hyperthermia radiating from the center of the wound peripherally for 10-12cm

On day 20, a nasal exudate was observed and aspirated for cytological examination. On day 21, vomiting occurred after tube feeding, and subcutaneous fluid administration was not absorbed well. CBC and serum chemistry profile were repeated on day 22 (Table 1). On day 23, blood was observed on the gastric tube following a feeding, and the seal's condition had deteriorated markedly, necessitating humane euthanasia.

Postmortem Examination

There was marked depletion of the subcutaneous and visceral adipose tissue, accompanied by mild-to-moderate skeletal and visceral muscle depletion (Figure 3). A mild-to-moderate, off-white exudate was noted in the right nostril. Culture revealed *Providencia rettgeri, Citrobacter freundii,* and normal naso-oropharyngeal flora that included *Enterococcus sp*.

The previously noted thoracic-dorsum, subcutaneous mass was noted externally as a thin, irregular scar. Deep along the left lateral, subcutaneous aspect of the thorax, were many small to moderate sized, adipose-like, grey foci. Cytologic examination of these foci revealed broad sheets of adipose cells, admixed with moderate numbers of bacterial cocci and bacilli, moderate numbers of neutrophils (many degenerate and band forms), monocytes, active macrophages (occasionally containing phagocytized bacteria and basophilic moderate detritus) and RBCs (Figure 4), indicating mixed panniculitis (cellulitis). These features likely were secondary to the original thoracic dorsum abscess. The left superficial cervical lymph node was moderately enlarged, also secondary to the abscess.

The lungs were inflated and light pink, excepting the caudal lobes that were collapsed, with deep-red, solid texture consistent with pneumonia or postmortem atelectasis. The bronchi contained a few nematodes (< 2cm) that were identified as *Parafilaroides decorum*. The liver and spleen were of normal coloration and size. The stomach contained nine oblong (3-5-inch) fleshy organisms, each having two trailing rear appendages, suggesting jellyfish and under-scoring the critical nutritional status of the seal. The abdomen contained 250ml of red-tinged effusion. Samples from lung, heart, spleen, liver, kidney, ileum, mesenteric & superficial cervical lymph nodes, were fixed in 10% formalin for histopathologic evaluation.

The urinary bladder was distended with ~35ml of light-brown urine. Urinalysis revealed specific gravity 1.053, pH 6.0, negative glucose & ketones, mild hematuria, bilirubin 3+, blood 2+, protein 1+; WBC 0-2/HPF, RBC 10-15/HPF, no bacteria, mucus or casts, epithelial cells 1+, 3-5 bilirubin crystals/HPF; amorphous debris; normal urobilinogen.

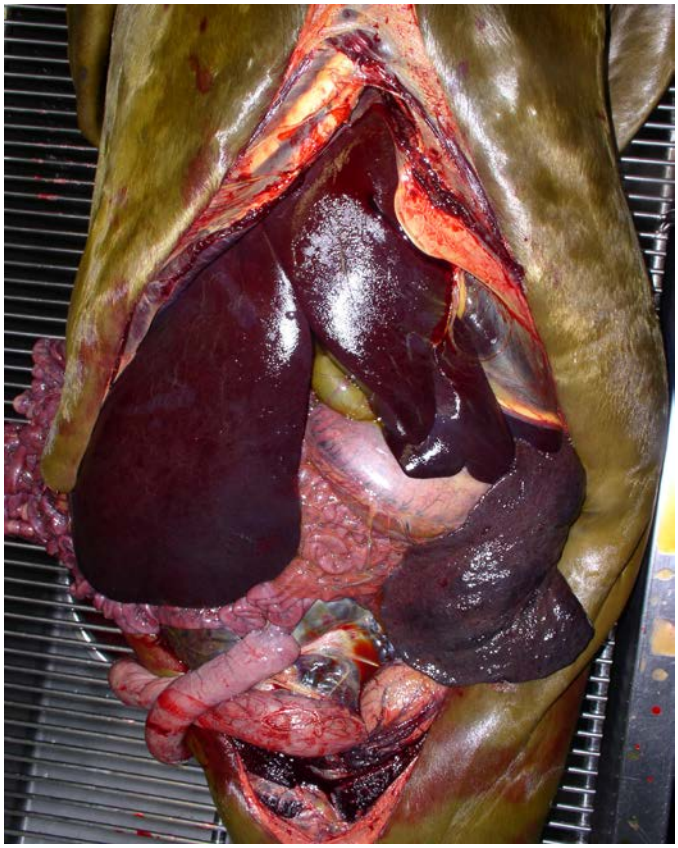

Figure 3. Depletion of subcutaneous-visceral adipose tissue and mild-moderate skeletal muscle depletion

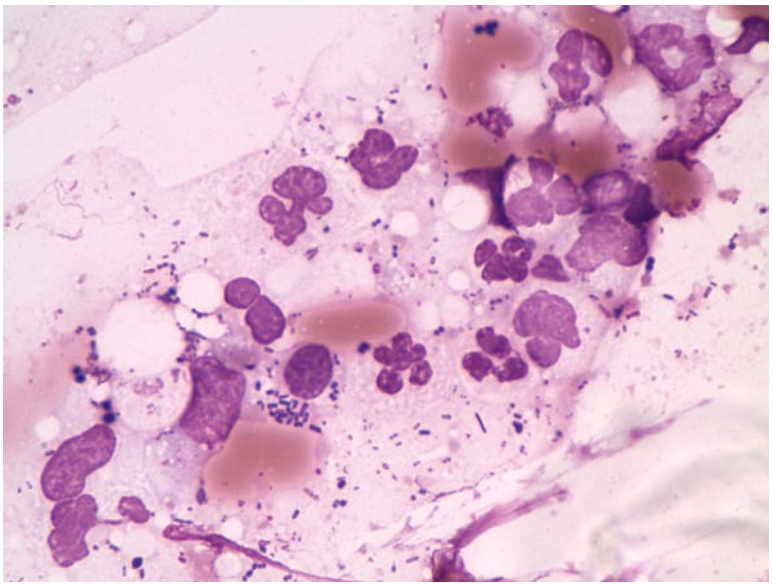

Figure 4. Cellulitis, multifocal, chronic-active, mixed-inflammation. Note multiple admixed bacteria

Low nucleated cellularity, occasional intact lymphocytes, and increased protein concentration characterize the peritoneal effusion as a modified transudate, common with sea lions in advanced malnutrition (IDEXX). Bile (3ml), Ascitis Fluid (5ml), and Urine (5ml) were taken for archiving (-30° F).

Histologic sections of lung, heart, kidney, and ileum were normal. The liver contained diffuse, mild-moderate, sinusoidal congestion; mild-moderate hepatocellular hemosiderosis; and multifocal, portal, dilated periarteriolar lymphatics (consistent with portal hypertension and heart failure). The left superficial cervical lymph revealed diffuse vascular congestion, packing of sinusoids with neutrophils and active macrophages, and depletion of normal lymphoid follicles. These features are consistent with chronic-active lymphadenitis, secondary to lung inflammation. The left superficial cervical lymph node evidently drained the thoracic dorsum abscess and its apparent daughter foci on the left thoracic subcutaneous area. The spleen revealed moderate numbers of active germinal centers and marked diffuse congestion (postmortem artifact). Medium-to-large sections of consolidating lung lesions contain marked-to-massive, diffuse, mural, septal and alveolar infiltration by neutrophils, monocytes, macrophages, and lymphoid cells; diffuse cuboidal, alveolar, epithelial hyperplasia; and moderate-marked vascular congestion and bronchio-alveolar hemorrhage.

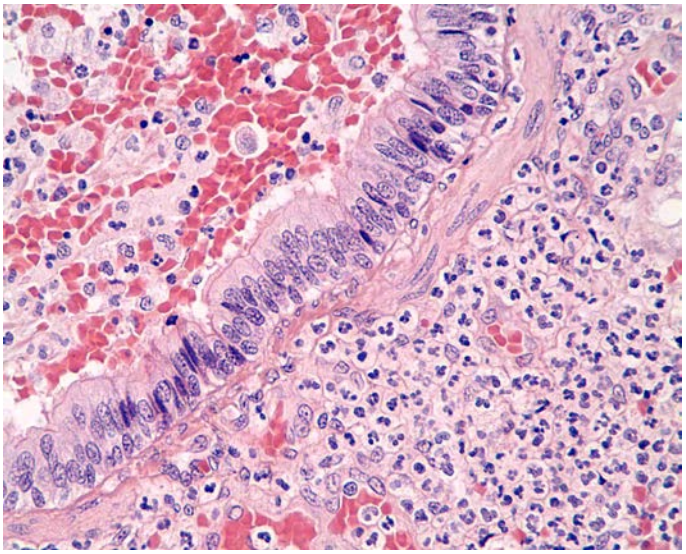

Figure 5. Pneumonia, multifocal-coalescing, severe, mixed, mononuclear-neutrophilic

Discussion

Halsted (1) summarized metabolic assessment of malnourished humans, observing that starvation is associated with hypo-metabolism, while the acute stress response causes hypermetabolism. It is interesting that hypometabolism and hyper-metabolism could co-exist, just as Halsted pointed out, in this young elephant seal with simultaneous advanced starvation and bacterial invasion of lung tissue. The relationship between the cutaneous-subcutaneous abscess and the pneumonia is speculative, although continuing subcutaneous cellulitis may have been a contributing factor. However, development of nasal exudate at day 20, followed by vomiting, poor absorption of subcutaneously administered fluid, rapidly worsening weakness, and hypothermia, are consistent with congestive heart failure. At necropsy, mild ascites, mild hematuria, and hepatic portal hypertension, also supported acute congestive heart failure.

Relatively stable erythrocytic metrics could partly reflect state of hydration, but also suggest against stem cell shifting toward leukocytic development in bone marrow. Further signs indicating no significant blood loss include minimal hema-turia, no gross blood in feces, modified transudate in the abdomen, and no cellulitis-associated hematoma.

Pneumonia likely caused the marked peripheral blood leukocytosis. Elevation of total WBC to 125,400/ul, with 82% neutrophils and 9% band neutrophils, initially suggests a regenerative response. Following the neutrophilic peak in

peripheral blood, declining but still elevated neutrophil numbers, along with fewer band neutrophils, could suggest either a degenerative shift or a stabilizing response to the infection. Lack of evidence for cell toxicity in peripheral blood tends to support the latter. Declining lymphocyte numbers and absence of eosinophils and basophils from peripheral circulation support a hypermetabolic stress response that would accompany a significant acute infection. An ongoing inflammatory process is expected to lead to monocytosis, as observed.

Lack of systemic inflammatory infiltrates could signal circulatory or chemotactic dysfunction, aberrant responses to cytokine production, or confinement of the infection. The latter is supported by observations at gross necropsy and by histological results. Relatively low but evidently stable total serum globulin, albeit not diagnostic, is compatible with some functioning level of humoral immunity. However, rapidly progressing terminal events could overshadow mean cell life spans and half-lives of a number of biochemical metrics, and thus degrees of interpretive caution are advisable.

Low serum alkaline phosphatase reflects growth cessation associated with starvation. Normally, growth cessation also is accompanied by lower serum phosphorus than we observed. Urine analysis, especially high specific gravity and low urine protein, document an adequate renal function that is compatible with subsequent renal histology. Thus, renal failure did not cause phosphorus retention. Severe metabolic acidosis can elevate serum phosphorus. It is likely that this seal's serum phosphorus reflects acid-base instability and muscle catabolism, counterbalanced by growth inhibition.

Liver-associated biochemical changes are compatible with congestion and hepatopathy, including elevations of ALT, AST, GGT, and bilirubin. Evidence of portal hypertension supports suspicion of heart failure. Elevated direct bilirubin and lower indirect bilirubin near termination suggest that hyperbilirubinemia was obstructive in the liver, consistent with observed histological sinusoidal congestion and lymphatic dilation. Low hemolysis index and indirect bilirubin support minimal hemolytic contribution. Bilirubin crystals in urine are expected effects of hyperbilirubinemia, and negative urobilinogen documents no enteric bile reabsorption.

Low serum urea nitrogen and creatinine reflect starvation processes that include advanced muscle wasting and lack of protein metabolism in the liver. Initially elevated serum CK, followed by rapid decline, also is compatible with advanced catabolism of skeletal muscle. At some point during near-terminal starvation, muscle catabolism ceases, which also is consistent with our observations of declining serum CK. At this point, death is inevitable.

Serum measures of energy metabolism provide an interesting view of the extreme status of starvation in this seal. Serum total protein reflects marginal adequacy of globulins (though not independently confirming functional adequacy) and increasing terminal rate of decline of serum albumin. The latter is consistent with loss of oral intake and loss of muscle-derived amino acid substrate for synthesis in the liver. Necropsy and clinical pathology did not reveal other causes for albumin loss from the body.

As expected, serum calcium declined in parallel to albumin, resulting from loss of albumin for calcium binding in peripheral blood. Declining serum glucose likely reflects loss of substrate for liver gluconeogenesis, but effects of lung infection could be contributory. Hypocholesterolemia is consistent with loss of substrate for liver synthesis, and also with prior systemic depletion. In earlier stages of starvation, hypercholesterolemia occurs, presumably resulting from shifting of substrate sources for energy metabolism. Dramatic elevation of serum triglycerides is compatible with the latter. Interestingly, the lipemia index of serum remained normal, suggesting that serum triglyceride, while elevated, remained below the level of visual detection. Some evidence of insulin resistance is evident in the two serum measures that were made. Insulin resistance is compatible with serious malnutrition and starvation.

Serum electrolytes represent the balance among hydration, systemic respiratory and metabolic contributions, tissue pathologies, and renal conservation-excretion functions. A blood gas analyzer was not available, but several observations are of interest with respect to starvation. Initial blood levels of sodium, chloride, RBC, hematocrit, hemoglobin, and osmolality, followed by declines, likely reflected initial dehydration and subsequent therapy. This observation suggests that hyponatremia and hypochloremia could have been caused by chronic starvation; hyponatremia also can be associated with low plasma osmolality and acute congestive heart failure (3), both of which were present. Serum potassium likely reflected

combined effects of continuing muscle loss and total body potassium depletion.

Urine pH 6.0 suggests that the kidneys were excreting excess hydrogen ion that precipitated reflex serum increase of total carbon dioxide (estimated as TCO_2 or HCO_3^-) to maintain electroneutrality, and also is consistent with histologically normal kidneys. Additionally, lung disease can result in respiratory acidosis; hypoalbuminemia artifactually decreases anion gap; and strong anion gap can increase during metabolic acidosis caused by unmeasured strong ions (2). However, since potentially competing and potentially reinforcing processes were noted in this rapidly deteriorating patient (1), it is difficult to state an unequivocal assessment of acid-base status. Brown-colored urine and bilirubinuria are normal occurrences in the elephant seal, and were not considered to be pathological complications.

Advanced starvation and inadequate protein intake, leading to protein catabolism with depressed protein synthesis, and liver complications of congestive heart failure, are mutually-reinforcing influences. Furthermore, congestive heart failure itself results in decreased blood flow rate through the lung field, possibly reinforced in this case by pulmonary consolidation. Cardiac histological lesions are not expected in acute cardiomyopathy secondary to starvation, particularly if wasting is rapid. Negative cardiac effects caused by electrolyte and acid-base derangement may have been contributory.

Mechanistically, when starvation or diseases such as severe chronic inflammation or cancer lead to cachexia, responses to corrective feeding often cease, sending an ominous signal for a negative outcome. Clinical markers for cachexia include cardiac wasting, hypocholesterolemia, lymphopenia, hypertriglyceridemia, and hypoalbuminemia (4, 5). The suspected underlying pathways involve broad activation of cytokines (protein products of inflammatory cells) that can exert negative effects on immunity, protein synthesis, proteolysis, and appetite stimulation, among many others (4, 5). Since clinical markers for diagnosis and monitoring of starvation bear some similarity to those that reflect cachexia, attending clinicians must be aware that some markers commonly having nutritional implications (cholesterol, triglycerides, albumin, and leukocytes) also may reflect much more serious metabolic perturbations that signal oncoming death.

Combined effects of the protein-energy “opposites” of starvation and severe organ inflammation can lead to the increasingly rapid protein catabolism and loss (1) that were observed terminally. Thus, a combination of subcutaneous and pulmonary inflammatory disease, and a hypermetabolic-catabolic stress response, probably exacerbated hypometabolic proteolysis of advanced starvation, worsening the cardiac complications and leading directly to death from severe acute cardiomyopathy and congestive heart failure. Quite possibly, broad cytokine induction played a significant mediating role in Dovahkin’s rapid deterioration. This case description illustrates the metabolic complexity of multiple and rapidly changing processes in a near-terminal starving marine mammal. In advanced deterioration of this nature, death often is inevitable.

References

1. Halsted CH. Malnutrition and Nutritional Assessment. In: Kasper DL, Braunwald E, Fauci AS, et al. (Eds.). Harrisons’ Principles of Internal Medicine, 16th ed. New York, McGraw-Hill Companies, Inc., pp. 411-415, 2008.
2. de Morais AH, Kaae J. Anion gap and strong ion gap: A quick reference. Vet Clin No Am 38(3):443-447, 2008.
3. de Morais AH, DiBartola SP. Hyponatremia: A quick reference. Vet Clin No Am 38(3):491-495, 2008.
4. Thomas DR. Distinguishing starvation from cachexia. Clin Geriatr Med 18:883-891, 2002.
5. Morley JE, Thomas DR, Wilson M-M G. Cachexia: pathophysiology and clinical relevance. Am J Clin Nutr 83:735-743, 2006.

Table 1. Serum Chemistry and Hematology

Serum Chemistry	Reference	(serum) Day 3	(serum) Day 19	(serum) Day 22	(aqueous) Day 23
Aklaline phosphatase U/L	108 – 454	162	124	89	96
Alanine transferase U/L	18 – 65	29	400	267	248
Aspartate transferase U/L	39 – 117	44	496	274	391
Creatinine phosphokinase U/L		672	216	51	175
Gamma glutamyl transferase U/L	22 – 136	186	229	178	168
Albumin g/dL	3.2 – 3.9	2.8	2.6	1.8	1.8
Total protein g/dL	6.6 – 9.9	5.7	6.4	4.8	4.7
Globulin g/dL	3.1 – 6.1	2.9	3.8	3.0	2.9
Total Bilirubin mg/dL	0.1 – 0.6	0.5	2.7	11.3	21.5
Direct bilirubin mg/dL		0.3	2.5	9.6	18.2
Urea nitrogen mg/dL	33 – 76	14	37	33	41
Creatinine mg/dL	0.2 – 0.8	0.5	0.5	0.4	0.6
Cholesterol mg/dL	100 – 347	228	194	108	83
Glucose mg/dL	128 – 189	163	91	82	64
Calcium mg/dL	10.2 – 12.8	10.0	8.9	7.5	7.6
Phosphorus mg/dL	6.6 – 9.9	6.5	8.1	6.9	6.9
TCO2 (HCO3) mEq/L		28	22	26	25
Chloride mEq/L	98 – 107	103	89	89	89
Potassium mEq/L	4.7 – 6.1	4.4	3.9	3.8	4.0
Sodium mEq/L	143 – 154	150	134	129	129
A/G ratio	1.0	0.97	0.70	0.60	0.60
B/C ratio		28.0	74.0	82.5	68.3
Indirect bilirubin mg/dL		0.2	0.2	1.7	3.3
Na/K ratio		34.1	34.4	33.9	32.3
Hemolysis index		N	1+	1+	2+
Lipemia index		N	N	N	N
Anion gap mEq/L	12-24 dog	23.4	26.9	17.8	19.0
AG corr for albumin (calc as dog)	12-24 dog	27.5	31.8	26.1	27.3
Strong Ion Gap (calc as dog)	0 – (-5) dog	-9.7	-14.6	-9.0	-10.2
Triglycerides mg/dL	76 – 301	111	167	469	597
Osmolality mosm/kg	285 – 295	314.1	286.3	274.3	276.2
Complete Blood Count					
WBC K/uL	10,600 – 28,500	20,200	125,400	77,800	82,700
RBC M/uL	2.6 – 3.3	3.70	3.48	3.19	3.37
Hemoglobin g/dL	16.2 – 24.2	27.3	24.7	22.7	23.7
Hematocrit (PCV) %	46 – 61	62.1	55.3	52.8	53.3
Mean cell volume fL	170 – 185	168	159	165	158
Mean cell hemoglobin pg	63 – 74	73.8	71.0	71.2	70.3
MCHC %	37 – 41	44.0	44.7	43.0	44.5
Neutrophils %	68 – 73	89	82.0	85.0	84.0
Absolute neutrophils n/uL	7,176 - 20,714	17,978	102,878	66,130	69,468
Lymphocytes %	23 – 37	7.0	4.0	4.0	3.0
Absolute lymphocytes n/uL	2,385 - 7,630	1,414	5,016	3,112	2,481
Monocytes %	3.8 – 12.0	4.0	5.0	3.0	10.0
Absolute monocytes n/uL	400 - 3400	808	6,270	7,002	8,270
Eosinophils %	0.9 – 2.5	0.0	0.0	0.0	0.0
Absolute eosinophils n/uL	100 - 795	0.0	0.0	0.0	0.0
Platlets (auto) K/uL		256	66	Clumped	Adequate